Analysis of Dual-Reflector Antenna for Radar Applications

A. Imani [1], M. Soleimani [1], and S. Amiri [2]

[1] Department of Electrical Engineering
Iran University of Science and Technology, Tehran, Iran
aliimani@iust.ac.ir, soleimani@iust.ac.ir

[2] Department of Electrical and Computer Engineering
Iranian Research Organization for Science and Technology, Tehran, Iran
amiri@irost.ir

Abstract ─ A dual-reflector antenna in millimeter wave frequency band is designed at center frequency of 35 GHz. The designed antenna has small size, low weight, fast beam scanning, high efficiency and high gain. Beam rotation of the proposed structure makes it useful for wide angle scanning in modern airborne radar systems. In the literature, beam rotation of similar structures used to be evaluated by two times of the twist-reflector rotation. For the first time, a nonlinear relationship is found between beam rotation and twist-reflector rotation. This nonlinear relation is theoretically extracted in this work. Furthermore, the designed antenna is simulated with a commercial full wave package. The results confirm that the designed goals are addressed. Moreover, the simulation results validate the extracted analytic relationship between beam rotation and twist-reflector rotation. In addition, low VSWR, low cross-polarization and good radiation pattern are observed.

Index Terms ─ Antenna radiation pattern, beam scanning, dual-reflector, feed horn, millimeter wave, polarization, trans-reflector, twist reflector.

I. INTRODUCTION

Airborne radar systems have many requirements such as small size, low weight, fast beam scanning, high efficiency and high gain. A reflector antenna is a good choice for low cost and high efficiency [1-4].

A dual-reflector antenna is compact, like a Cassegrain reflector antenna; but, it delivers high efficiency, high gain and low sidelobe levels of a prime-focus reflector. The dual-reflector antenna, as a compact option for the Cassegrain, has performed more comparably to a prime-focus reflector antenna. The antennas in millimeter wave frequency bands can have physically small sizes; yet, they can achieve gains in excess of 30 dB [5-11].

This antenna is composed of three parts: the main reflector (twist reflector), sub-reflector (trans-reflector) and feed horn. Details of the design method of a dual-reflector antenna and its parts are explained below.

Trans-reflector is a parabola structure which acts as both a reflector antenna and a radome. The trans-reflector is made of conductive-strip grating embedded in a shaped dielectric molding [12]. It is easy to see that a large sub-reflector blocks effective area of the main reflector (aperture blocking phenomenon). However, if only one polarization is permissible, this adverse effect can be considerably decreased.

Consider the antenna in transmitting mode, as in Fig. 2. A feed horn antenna with linear polarization illuminates the trans-reflector that its electric field vector is aligned parallel to the conductive strip grating. The strips are arranged orderly beside each other so that the trans-reflector collects and then reflects the incident wave with considerable reduction in escaping waves to the space. While the twist-reflector receives the reflected radiation from the trans-reflector, the twist-reflector rotates field vector 90 degrees and then redirects it toward the trans-reflector. The electric field polarization is perpendicular to the trans-reflector's strips grating direction, and then it passes through the trans-reflector into the space with an inconsiderable loss.

The attenuation versus frequency diagram for oxygen and water vapor is shown in Fig. 1 [13]. This diagram shows some minimum attenuation at special frequencies such as 35, 94 and 225 GHz. Here, the antenna design frequency is selected 35 GHz.

In this article, analysis, design, simulation and optimization of dual-reflector antenna is described. A dual-reflector antenna is designed in millimeter wave frequency band. The theory and relations of this design are also extracted in this work. Then, it is focused on design methods of antenna parts, including the trans-reflector, twist-reflector and feed horn.

Submitted On: April 22, 2014
Accepted On: October 22, 2015

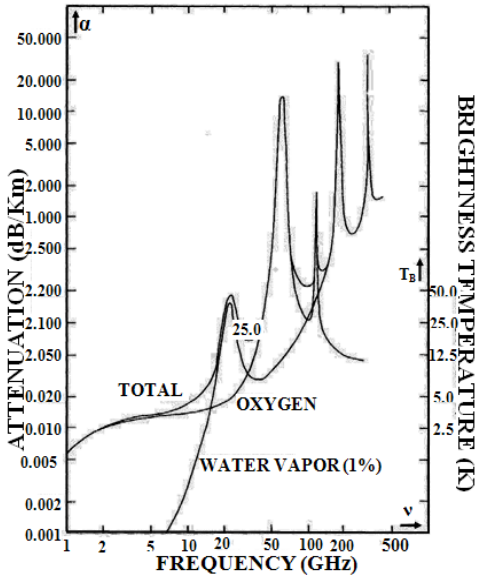

Fig. 1. Attenuation versus frequency diagram for oxygen and water vapor.

II. ANTENNA CONFIGURATION

The proposed antenna is divided to three parts: a feed horn, a trans-reflector, and a twist-reflector as revealed in Fig. 2. The design method of any part is discussed below.

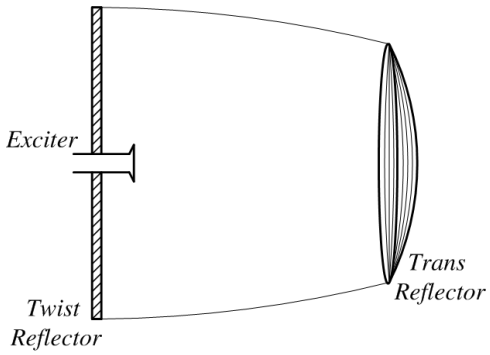

Fig. 2. Configuration of the proposed antenna.

A. Feed horn design

The feed horn antenna is designed specifically for the millimeter wave frequency band for which, the most essential requirements are as follows: 1- to keep the input return loss high throughout the operating frequency interval, and 2- to optimize the E- and H-plane beam width maximizing performance (gain). Figure 3 shows the designed horn antenna and its dimensions.

Dimensions of the designed horn antenna are a=9 mm, b=10 mm, and l=20 mm as noted in Fig. 3. The simulation results for return loss of the antenna are shown in Fig. 4 which confirms the satisfactory return loss suitable for feeding.

Figure 5 demonstrates the simulated power radiation patterns at the center frequency (35 GHz) in both E- and H-planes.

Since the horn antenna has a phase center, the best performance of dual-reflector antenna can be achieved when the phase center of horn antenna is located at the trans-reflector focal point.

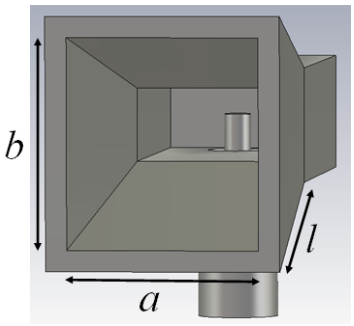

Fig. 3. Designed horn antenna.

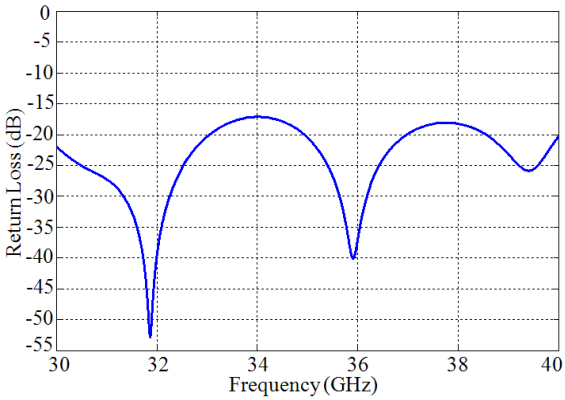

Fig. 4. Return loss of the horn antenna.

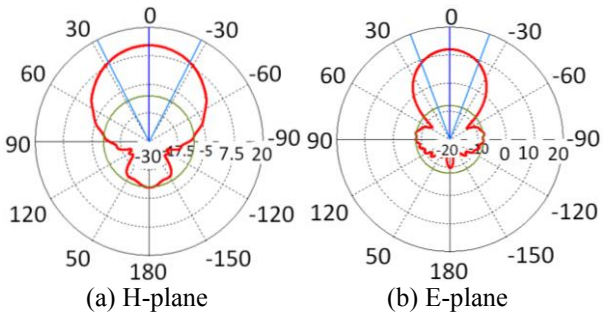

Fig. 5. Radiation pattern of the horn antenna for 35 GHz.

B. Trans-reflector design

The trans-reflector has a periodic structure which includes a set of embedded conductive strips grating inside a dielectric layer, as shown in Fig. 6. This structure does two functions: first, it acts as a reflector which collocates feed-horn radiation and second, it is a

radome to collocate the returned energy from the twist-reflector. The function of the trans-reflector is almost dependent on the polarization of the incident electric field.

Whenever the electric field is parallel to the strips (as in Fig. 6) we call it a reflect-polarized because the field reflects; otherwise we call it a thru-polarized because the field passes through the strip grating. Since the grating has not a continuous conductive surface, there is some loss in the reflected polarization. For the thru-polarized signal, the trans-reflector acts like a radome.

This structure has a parabolic shape. The dimensions of the proposed antenna are as follows: W_t=1 mm and S_t=1 mm, where W_t is the strip width and S_t is the space between the strips.

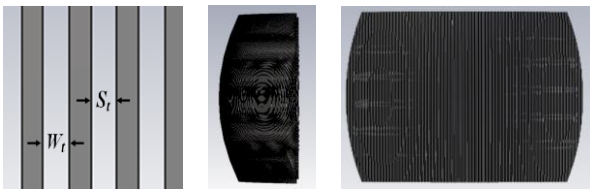

(a) Strip grating (b) Side view (c) Front view

Fig. 6. Trans-reflector structure.

C. Twist-reflector design

A planar reflection structure has been used to rotate the incident electromagnetic wave. For economical reasons, a dielectric twist-reflector is used: a quarter-wave, ground-plane-backed and dielectric layer printed with conductive strip grating.

Figure 7 shows the twist-reflector and a vertically polarized incident electric field on its conductive strips grating. The conductive strips and the incident electric field are making 45 degrees angle.

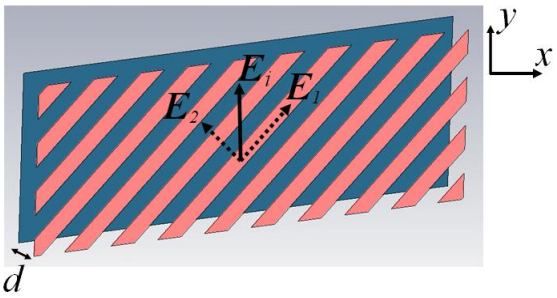

Fig. 7. Twist-reflector structure.

The incident electric field can be decomposed into parallel and perpendicular components with respect to the strips which will be reflected and transmitted, respectively. The transmitted perpendicular component travels through the dielectric substrate and will be reflected by the ground plane.

Assume the incident electric field vector is y-directed,

$$E_i = E_0\, e^{-j\beta z}\, \hat{y}, \tag{1}$$

where E_0 is the incident electric field amplitude, β is the wave number and z is the propagation direction. Then, the parallel and perpendicular components are:

$$\begin{aligned} E^i_{r1} &= E_i \cos\theta\left(\hat{x}+\hat{y}\right) = E_0\, e^{-j\beta z}\cos\theta \quad \left(\hat{x}+\hat{y}\right), \\ E^i_{t1} &= E_i \cos\theta\left(-\hat{x}+\hat{y}\right) = E_0\, e^{-j\beta z}\cos\theta\,\left(-\hat{x}+\hat{y}\right), \end{aligned} \tag{2}$$

where E^i_{r1} is parallel component and E^i_{t1} is perpendicular component and their reflection of the ground plane are:

$$\begin{aligned} E^r_{r2} &= E_i \cos\theta\left(\hat{x}+\hat{y}\right) = E_0\, e^{+j\beta z}\cos\theta\left(\hat{x}+\hat{y}\right), \\ E^r_{t2} &= E_i\, e^{-j\beta d\times 2}\cos\theta\left(\hat{x}-\hat{y}\right) \\ &= E_0\, e^{+j\beta z}\, e^{-j\beta d\times 2}\cos\theta\,\left(\hat{x}-\hat{y}\right), \end{aligned} \tag{3}$$

where E^r_{r2} is the reflection of E^r_{r1}, E^r_{t2} is the reflection of E^i_{t1} and d is the substrate thickness. Therefore, the total field is:

$$\begin{aligned} E^r_t &= E^i_{r1} + E^r_{t2} \\ &= E_0\, e^{j\beta z}\cos\theta\left(\hat{x}+\hat{y}+e^{j\beta d\times 2}\left(-\hat{x}+\hat{y}\right)\right) \\ &= E_0\cos\theta e^{j\beta z}\left\{\hat{x}\left(1-e^{-j2\beta d}\right)+\hat{y}\left(1+e^{-j2\beta d}\right)\right\}, \end{aligned} \tag{4}$$

where E^r_t is the total reflected field.

To transmit the reflected wave through the trans-reflector, the electric field polarization must be horizontal (perpendicular to the trans-reflector conductive strips grating). Therefore, the reflected electric field polarization must be rotated 90 degrees relative to the incident electric field polarization.

By choosing the strip width and spacing and the substrate thickness properly, the phase difference between the two electric field components can be set as 180 degrees. Thus, rotating the total reflected electric field 90° relative to the incident electric field.

So, the electric field component in y direction must be zero:

$$\begin{aligned} &1+e^{-j2\beta d}=0 \;\Rightarrow -2\beta d=-\pi \quad , \quad \beta=\frac{2\pi}{\lambda} \\ &2\times\frac{2\pi}{\lambda}\times d=\pi \;\Rightarrow\; d=\frac{\lambda}{4}. \end{aligned} \tag{5}$$

Therefore, the substrate thickness is λ/4. The dual-reflector antenna dimensions are much larger than the operational wavelength. Therefore, the edge effects can be ignored.

III. THE RELATION BETWEEN THE TWIST-REFLECTOR ROTATION ANGLE AND THE BEAM ROTATION ANGLE

The antenna coordination is shown in Fig. 8, where $-z$ is the direction of the incident wave and the normal unit vector on the twist-reflector is:

$$\hat{n}=\cos(el)\sin(az)\hat{x}+\sin(el)\hat{y}+\cos(az)\cos(el)\hat{z}, \quad (6)$$

where the *az* and *el* are rotation angles in azimuth and elevation directions, respectively.

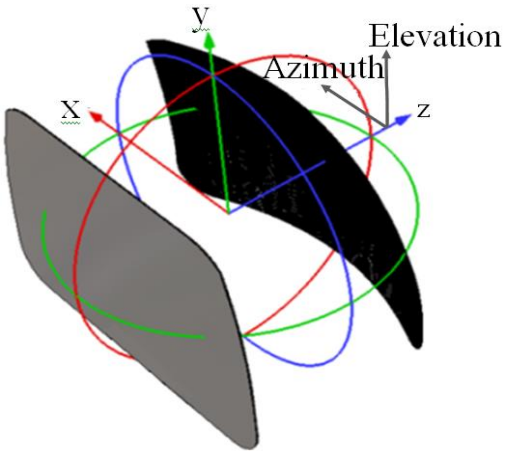

Fig. 8. Antenna coordination.

The propagation direction vector can be into the tangential and perpendicular components as:

$$\hat{I}_t=\left(\hat{I}.\hat{n}\right)\hat{n}, \quad (7)$$

$$\hat{I}_p=\hat{I}-\hat{I}_t=\hat{I}-\left(\hat{I}.\hat{n}\right)\hat{n}, \quad (8)$$

where I_t and I_p are the tangential and perpendicular components, respectively.

As is revealed in the Fig. 9, the perpendicular vector direction remains the same for both incident and reflection states; but, the tangential component direction inverses from the reflection state to the incident state. Therefore,

$$\begin{aligned}\hat{r}&=\hat{I}_p-\hat{I}_t\\&=\hat{I}-\left(\hat{I}\cdot\hat{n}\right)\hat{n}-\left(\hat{I}\cdot\hat{n}\right)\hat{n}=\hat{I}-2\left(\hat{I}\cdot\hat{n}\right)\hat{n},\end{aligned} \quad (9)$$

where $\hat{r}$ is the reflection vector direction. By use of equation (6) into equation (9),

$$\begin{aligned}\hat{r}&=\sin(2az)\cos^2(el)\hat{x}+2\cos(az)\cos(el)\sin(el)\hat{y}\\&+\left(a\cos^2(az)\cos^2(el)-1\right)\hat{z},\end{aligned} \quad (10)$$

where *az* and *el* are twist-reflector rotation angles in azimuth and elevation directions, respectively. Then, the beam vector direction is:

$$\begin{aligned}\hat{r}&=\cos(el_r)\sin(az_r)\hat{x}+\sin(el_r)\hat{y}\\&+\cos(az_r)\cos(el_r)\hat{z},\end{aligned} \quad (11)$$

where the az_r and el_r are the beam rotation angles in azimuth and elevation directions, respectively.

Using equations (10) and (11), the beam rotation angles are:

$$el_r=\sin^{-1}\left(2\cos(az)\cos(el)\sin(el)\right), \quad (12)$$

$$az_r=\tan^{-1}\left[\frac{\sin(2az)\cos^2(el)}{2\cos^2(az)\cos^2(el)-1}\right]. \quad (13)$$

In this state, the beam rotation angle will clear when the *az* and *el* is known.

Assuming (az_r,el_r) as the antenna vector direction, as shown in the Fig. 8, the normal vector is:

$$\hat{n}=\frac{\hat{r}-\hat{I}}{\left|\hat{r}-\hat{I}\right|}, \quad (14)$$

$$\begin{aligned}\hat{n}=&\frac{\sqrt{2}\cos(el_r)\sin(az_r)}{2\sqrt{\cos(az_r)\cos(el_r)+1}}\hat{x}+\frac{\sqrt{2}\sin(el_r)}{2\sqrt{\cos(az_r)\cos(el_r)+1}}\hat{y}\\&+\frac{\sqrt{2\cos(az_r)\cos(el_r)+2}}{2}\hat{z}.\end{aligned} \quad (15)$$

The normal vector direction in azimuth and elevation rotation angles (*az*, *el*) is:

$$\begin{aligned}\hat{n}=&\cos(el)\sin(az)\hat{x}+\sin(el)\hat{y}\\&+\cos(az)\cos(el)\hat{z}.\end{aligned} \quad (16)$$

Equations (15) and (16) give the antenna rotation angles:

$$el=\sin^{-1}\left(\frac{\sqrt{2}\sin(el_r)}{2\sqrt{\cos(az_r)\cos(el_r)+1}}\right), \quad (17)$$

$$az=\tan^{-1}\left(\frac{\frac{\sqrt{2}\cos(el_r)}{\sqrt{\cos(az_r)\cos(el_r)+1}}\times}{\frac{\sin(az_r)}{\sqrt{2\cos(az_r)\cos(el_r)+2}}}\right). \quad (18)$$

According to the above equations, the twist-reflector rotation angle versus beam rotation angle in azimuth and elevation directions are indicated in Fig. 10, in which the difference between the linear state (mirror law) and nonlinear state (the above equations) is clear.

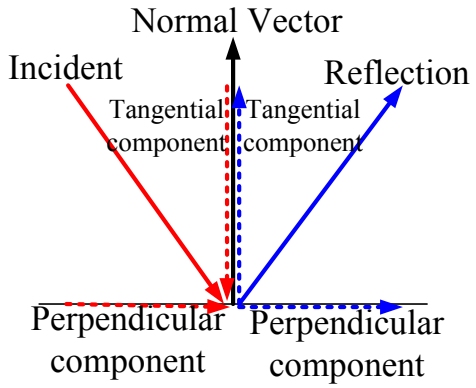

Fig. 9. Incident and reflection state.

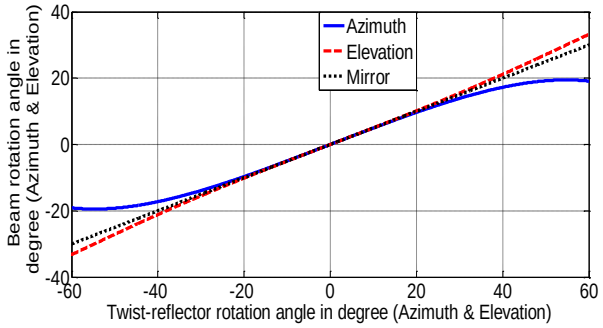

Fig. 10. The twist-reflector rotation angle versus beam rotation angle in azimuth and elevation.

IV. SIMULATION AND RESULTS

Configuration of the dual-reflector antenna is given in Fig. 11. The proposed antenna is simulated with commercially available packages such as CST microwave studio in the operating frequency range. This antenna has very high gain, narrow beam-width and very good sidelobe level. The simulated radiation pattern of the dual-reflector antenna is shown in Fig. 12.

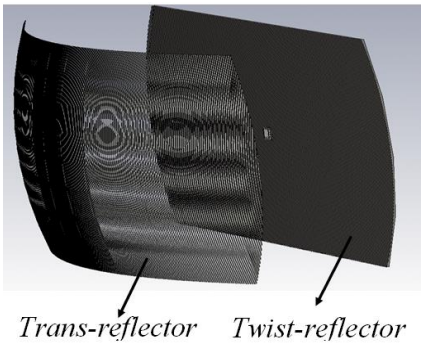

Fig. 11. Configuration of dual-reflector antenna.

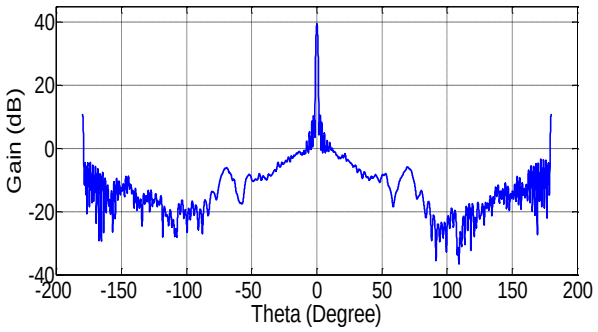

Fig. 12. Simulated radiation pattern at frequency of 35 GHz.

This antenna has fast beam scanning capability. The radiation patterns for various azimuth scan angles (0°, 30° and 60°), *el*=0, and for various elevation scan angles (0°, 20° and 30°), *az*=0, are respectively shown in Figs. 13 and 14 that their specifications are numerically listed in Table 1.

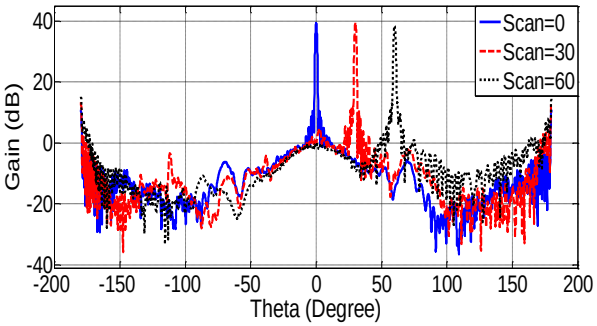

Fig. 13. Radiation pattern in azimuth scan.

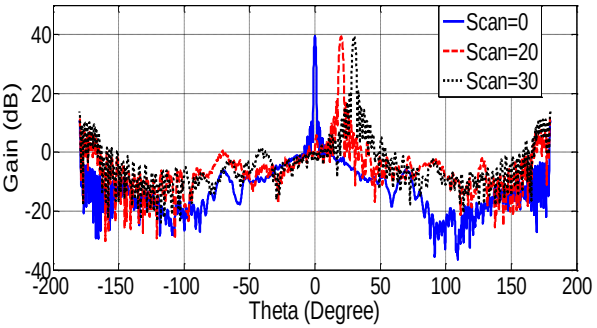

Fig. 14. Radiation pattern in elevation scan.

Table 1: Specification of radiation pattern

Scan Angle (degree)	0°	30°	60°
Gain (dB)	39.4	39.2	38.5
HPBW (degree)	1.2	1.2	1.3
S.L.L	-28.5	-26.1	-23.3

The linear and nonlinear equations (Eqs. 12 and 13) are equal in a specific circumstance whenever *el*=0 or *az*=0. Otherwise, if the *az* and *el* angles are not zero simultaneously, the radiation pattern will become different for two mentioned equations. For instance, if *el*=10 and *az*=15 are putted in linear and nonlinear equations, results will be el_r=20 and az_r=30, el_r=19.29 and az_r=30.91 respectively.

Regarding to simulation results, the radiation pattern is shown in Fig. 15 for two elevation planes, el_r=20 and el_r=19.29. It is apparent that the peak of pattern is located in el_r=19.29 rather than el_r=20. This trend is also repeated for two azimuth planes, az_r=30 and az_r=30.91 in Fig. 16. A plane included the peak of pattern is desirable. Therefore, the proposed nonlinear equation is absolutely correct. For more clarifications of Figs. 15 and 16, specifications of the radiation patterns are numerically listed in Table 2.

Regarding to the Table 2, the gain is decreased 6.3 dB in the plane az_r=30 rather than az_r=30.91 in azimuth direction, and 1.3 dB in the plane el_r=20 rather than el_r=19.29. As a result, the beam scanning is not correct without the using of nonlinear equation for this structure.

Figurre 17 shows simulated co- and cross-polar far-field radiation patterns at frequency of 35 GHz. From this figure, it is seen that the designed antenna exhibits low cross-polarization which its level is less than -40 dB.

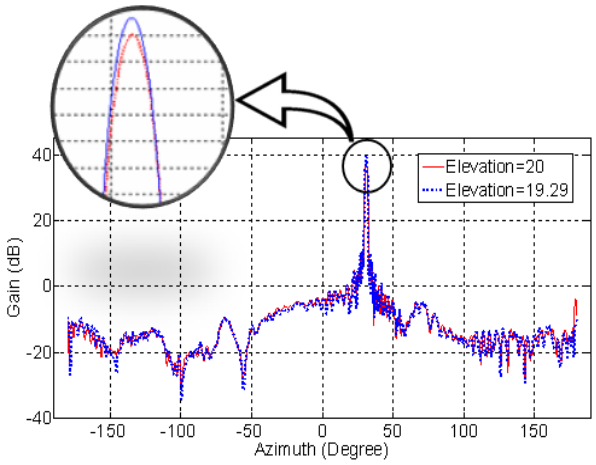

Fig. 15. Radiation pattern in elevation scan.

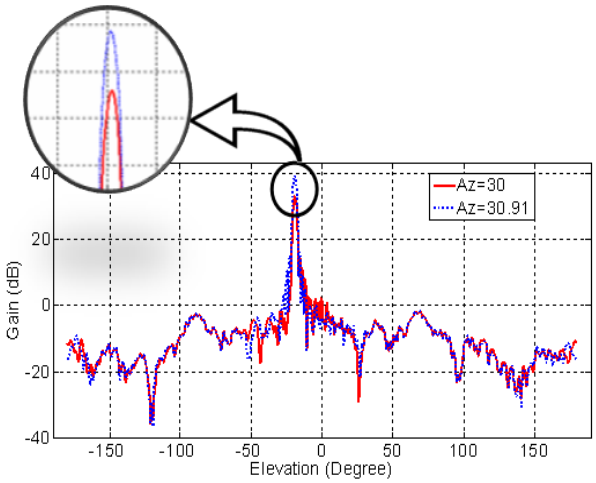

Fig. 16. Radiation pattern in azimuth scan.

Table 2: Specification of radiation pattern

Direction / Specification	In Azimuth		In Elevation	
Angle (degree)	30	30.91	20	19.29
Gain (dB)	33	39.3	38	39.3
HPBW(degree)	2.2	2.2	1.3	1.3
SLL (dB)	-18.4	-23.2	-28.3	-28.6

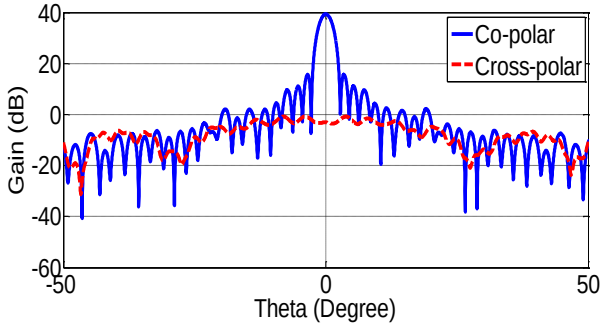

Fig. 17. Comparison of co- and cross-polarization.

V. CONCOLUSION

In this paper, a dual-reflector antenna has been presented at center frequency of 35 GHz. This antenna is a type of Cassegrain which equipped with two reflectors: a flat (twist-reflector) and a parabola (trans-reflector). A new formula is extracted in the relation between the twist-reflector mechanical movement and the beam rotation angle. Without this formula the beam scanning is not correct. This antenna has small size, low weight, fast beam scanning, wide angle beam scanning, low cross-polarization, high efficiency and high gain. The designed antenna has good far-field radiation characteristics in the entire operating bandwidth in both azimuth and elevation directions. The antenna presents beam scanning capability ±60° in azimuth and ±30° in elevation by mechanical movement of the twist-reflector. Based on these characteristics, the proposed antenna can be useful for airborne radar systems and millimeter wave applications.

REFERENCES

[1] J. Shalit, "The manufacture of airborne Cassegrain antenna," *IEEE Symposium on Mechanical Engineering in Radar*, pp. 220-224, Nov. 1977, IEEE Pub 77CH1250-0-AES.

[2] B. L. Lewis and J. P. Shelton, "Mirror scan antenna technology," *International Radar Conference*, pp. 279-283, Apr. 1980.

[3] D. D. Howard, D. C. Cross, and H. Poor, "Mirror-antenna dual band lightweight mirror design," *IEEE Transaction on Antenna and Propagation*, vol. 33, pp. 286-294, Mar. 1985.

[4] D. C Cross, D. D. Howard, and J. W. Titus, "Mirror-antenna radar concept," *Microwave Journal*, vol. 29, pp. 323-324, May 1986.

[5] K. S. Kellejer and G. Hyde, *Reflector Antennas*, in R. C. Johnson and H. Jasik (eds.), Antenna Engineering Handbook, Second Edition, New York, McGraw-Hill, ch. 17, p. 29, 1984.

[6] E. L. Holzman, "Transreflector antenna design for millimeter-wave wireless links," *IEEE Antennas*

and Propagation Magazine, vol. 47, no. 5, pp. 9-22, Oct. 2005.

[7] H. Haiden, L. Xiumei, and C. Zhangliang, "Design of fast-scanning millimeter-wave monopulse antenna," *International Conference on Radar*, pp. 1-4, Oct. 2006.

[8] Z. Hussein, K. Green, E. Im, and S. Durden, "Design of offset reflector with elliptical flat scan mirror and its applications to a dual-frequency, dual-polarization airborne rain radar observation," *IEEE International Symposium on Antennas and Propagation Society*, vol. 1, pp. 642-645, 2002.

[9] L. K. De Size and J. F. Ramsay, *Reflecting Systems*, in R. C. Hansen (ed.), Microwave Scanning Antennas, Los Altos, CA, Peninsula Press, pp. 127-128, 1985.

[10] C. A. Cochrane, *High Frequency Radio Aerials*, US Patent 2,736,895, Feb. 28, 1956.

[11] E. O. Houseman, "A millimeter wave polarization twist antenna," *IEEE International Symposium on Antennas and Propagation Society*, vol. 16, pp. 51-54, May 1978.

[12] R. A. Vandendolder and G. D. Winslow, *Insert Mold Process for Forming Polarizing Grid Element*, US Patent 6,246,381, June 12, 2001.

[13] http://www.propagation.gatech.edu/ECE6390/project/Fall2012/Team07/Space%20Reach%20Website/index_files/Page785.htm.

Ali Imani was born in Iran in 1982. He received the B.S. degree in Electrical Engineering from Tabriz University, Tabriz, Iran, in 2006 and M.S. degree in Electrical Engineering from Shahed University, Tehran, Iran, in 2009. He is currently working toward the Ph.D. degree at Iran University of Science and Technology, Tehran, Iran. His research interests include slot antennas, wideband antennas, millimeter-wave antennas, analysis and design of microstrip antennas, radar systems and electromagnetic theory.

Mohammad Soleimani received the B.S. degree in Electrical Engineering from the University of Shiraz, Shiraz, Iran, in 1978 and the M.S. and Ph.D. degrees from Pierre and Marie Curio University, Paris, France, in 1981 and 1983, respectively.

Currently, he is a Professor with the Iran University of Sciences and Technology, Tehran, Iran. His research interests include computational electromagnetic and antennas.

Shervin Amiri was born in Iran in 1966. He received the B.S., M.S., and Ph.D. degrees in Electrical Engineering from the Iran University of Science and Technology, Tehran, in 1988, 1994, and 1999, respectively. He is currently an Assistant Professor in the Electrical and Computer Engineering Department of IROST. His research interests include satellite communication and microwave and millimeter-wave antennas.